A Numerical Study of the Thermal and Electrical Performance of Water-Based PVT Collectors with Varying Configurations

Rudi Darussalam
Department of Electrical Engineering, Universitas Indonesia, Depok, West Java, Indonesia
rudi.darussalam21@ui.ac.id

Iwa Garniwa
Department of Electrical Engineering, Universitas Indonesia, Depok, West Java, Indonesia
iwa@eng.ui.ac.id (corresponding author)

Chairul Hudaya
Department of Electrical Engineering, Universitas Indonesia, Depok, West Java, Indonesia
c.hudaya@eng.ui.ac.id (corresponding author)

Ahmad Fudholi
Research Center for Energy Conversion Technology, National Research and Innovation Agency (BRIN), Tangerang Selatan, Indonesia
ahmad.fudholi@brin.go.id

Received: 20 January 2026 | Revised: 28 February 2026 and 25 March 2026 | Accepted: 1 April 2026

 DOI: https://doi.org/10.48084/etasr.17653

ABSTRACT

This study evaluates the performance of water-based Photovoltaic Thermal (PVT) systems with three absorber collector configurations: twin spiral, direct, and oscillatory. Simulations were carried out using the Computational Fluid Dynamics (CFD) ANSYS software in steady-state conditions by considering the influence of variations in water mass flow rate (0.015 kg/s – 0.055 kg/s) and solar irradiance levels (600 W/m², 700 W/m², 900 W/m², and 1000 W/m²). The results showed that the absorber configuration significantly influenced PV cooling and energy performance. Among the three designs, the twin spiral configuration provided the best overall performance. At 900 W/m² and 0.02 kg/s, the twin spiral configuration reduced the PV temperature to 43.38 °C, compared with 56.59 °C for the direct configuration and 43.84 °C for the oscillatory configuration. Under the same condition, it achieved an electrical efficiency of 17.25% and a thermal efficiency of 77.37%, compared with 16.00% and 77.44% for the direct configuration, and 17.21% and 77.35% for the oscillatory configuration. The highest electrical efficiency obtained in this study was 18.06%, achieved by the twin spiral configuration at 600 W/m² and 0.055 kg/s. These findings indicate that the twin spiral absorber offers the most favorable balance between PV cooling and combined thermal-electrical performance among the investigated configurations.

Keywords-photovoltaic thermal systems; collector configuration; mass flow rate; solar irradiance; thermal performance; electrical efficiency

I. INTRODUCTION

The high dependence on fossil fuels to meet increasing global energy demand has led to serious environmental problems, including climate change and increased greenhouse gas emissions [1, 2]. To address these issues, environmentally friendly renewable energy is needed. Among various renewable energy sources, solar energy holds promise due to its abundant availability, pollution-free nature, and ability to be utilized in almost any region [3]. Photovoltaic (PV) technology harnesses solar energy to generate electrical energy. However, PV modules have a significant limitation: their electrical conversion efficiency decreases with increasing cell temperature. Increasing the temperature of PV cells above 25°C can cause a decrease in electrical efficiency, with an estimated decrease of around 0.3–0.5% for every 1°C increase [4, 5]. This condition causes the performance of PV modules to decrease, especially in tropical and hot climates.

To overcome this problem, a Photovoltaic Thermal (PVT) system was developed, which combines PV modules with thermal collectors into a single device [6, 7]. The PVT system can actively cool PV modules to lower cell temperatures while simultaneously utilizing the resulting heat as thermal energy. This hybrid approach not only improves electrical efficiency but also generates heat energy that can be used for various applications, such as water heating, air conditioning, distillation, and more [8]. In addition, the PVT system has advantages in terms of land use efficiency, lower installation costs, and higher energy efficiency compared to separate thermal and PV systems [9, 10]. Furthermore, adding an absorber to the PV module, as implemented in PVT collectors, provides a cooling effect that enhances the electrical energy conversion efficiency [11, 12]. To optimize solar energy capture and simultaneously generate thermal and electrical energy, a PVT system must include a PV module, absorber, working fluid, insulation, and other essential components [13, 14].

The classification of PVT systems is generally determined by two main aspects: the type of working fluid used and the collector construction design. In existing configurations, various types of working fluids can be applied, such as air, water, nanofluids, and refrigerants [15, 16]. Authors in [17] claimed that the use of water as a working fluid is more effective because it has a higher heat capacity and thermal conductivity, thereby increasing heat transfer performance in the system. Meanwhile, classification based on collector construction can be made according to the type of tube used, heat pipe configuration, and variations in absorber plate design [18, 19]. This approach allows the development of PVT systems that are more flexible and can be adapted to specific operational needs and conditions.

The performance of a PVT system is significantly influenced by the collector design, particularly the thermal absorber configuration and the coolant flow path. The effectiveness of the absorber in transferring heat from the PV module to the working fluid plays a major role in increasing the thermal and electrical efficiency of the system [20, 21]. In-depth studies have been conducted to develop various approaches capable of increasing the rate of heat transfer in PVT systems. The strategies implemented to optimize this heat exchange process are known as heat transfer augmentation techniques [22]. In general, these techniques are divided into two main categories: active and passive methods. Active methods use external devices, such as pumps and fans, to increase fluid flow rates, thereby achieving more effective heat transfer. In contrast, passive methods rely on internal modifications to the system, such as adding fins, changing the tube shape, or using twisted tubes, which aim to create turbulence and expand the heat transfer area without requiring additional energy.

Although many studies have reported performance improvements in PVT collectors, direct comparison across the literature remains difficult because the investigated designs are typically evaluated under different boundary conditions and objectives. For example, authors in [23] focused on the addition of inner fins and reported thermal enhancement and PV temperature reduction, but the comparison was based on a different heat-transfer augmentation approach rather than an equivalent channel-path geometry. Authors in [24] compared zigzag and spiral-type arrangements with emphasis on the balance between thermal efficiency, electrical efficiency, and pressure drop, while authors in [25] reported field-test results for spiral, web, and direct-flow designs under site-specific outdoor conditions in Oman. In addition, authors in [26] numerically compared multiple serpentine layouts and highlighted the role of multi-inlet design on thermal/electrical performance and pressure distribution. Because these studies differ in collector geometry, materials, operating conditions, and evaluation focus, the reported results cannot be used for an objective one-to-one assessment of absorber flow-path performance. Unlike a straight direct configuration, the oscillatory configuration introduces periodic changes in flow direction, which are expected to enhance local mixing and disrupt thermal boundary layer development, thereby improving local heat transfer. At the same time, compared with more aggressive passive enhancement strategies, the oscillatory pattern provides a simpler geometry that can be evaluated under the same collector area and boundary conditions as the twin spiral and direct configurations. Therefore, a systematic comparison under uniform conditions is still needed to isolate the effect of absorber configuration on thermal uniformity, PV cooling behavior, and overall PVT performance.

This study numerically compares three collector configurations: twin spiral, direct, and oscillatory under identical collector area, material assumptions, and boundary conditions, while varying solar irradiance and water mass flow rate. The objective is to provide a controlled and standardized evaluation of how flow-path geometry affects temperature distribution in the collector and PV surface, outlet-water temperature, and the resulting thermal and electrical performance of a water-based PVT system.

II. METHOD

This study analyzed and compared the performance of PVT systems with different collector configurations, namely twin spiral, direct, and oscillatory. The analysis was carried out using ANSYS Fluent software, a branch of Computational Fluid Dynamics (CFD) software. The simulation considered the effects of changing solar radiation levels and water mass flow rates – two factors that impact the thermal and electrical performance of the PVT system. The main parameters analyzed include the PV module temperature, which affects the electrical efficiency, and the outlet water temperature, which influences the thermal efficiency of the system.

A. Model Geometry

Several layers make up the PVT system's geometry, as illustrated in Figure 1. Table I lists the dimensions of the PVT collector along with the thermophysical parameters of each component [26]. The thermophysical properties of the solid PVT layers were assumed to be constant because the study focuses on a comparative evaluation of absorber configurations under identical operating conditions. Figure 2 shows the front view of the three different collector absorber designs: twin

spiral, direct, and oscillatory. The collector area for all three configurations is the same, namely 1.17 m².

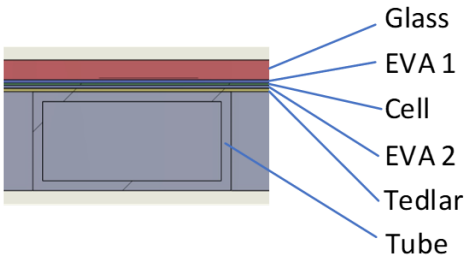

Fig. 1. Layers of the PVT system.

TABLE I. PROPERTIES OF THE LAYERS PVT SYSTEM

Name	Thickness (m)	Thermal conductivity (W/mK)	Density (kg/m³)	Heat capacity (J/Kg K)
Glass	0.003	2	2450	500
EVA	0.0005	0.35	960	2090
Solar cells	0.0003	148	2329	700
Tedlar	0.0005	0.2	1200	1250
Aluminum	0.002	202.4	2719	871

B. Boundary Condition

The boundary conditions used in the simulation are determined to represent the real operating conditions of the PVT system. Some of the boundary conditions applied include: the variations in the simulated solar radiation levels are 600 W/m², 700 W/m², 900 W/m², and 1000 W/m². The water mass flow rate is varied in the range of 0.015 kg/s to 0.055 kg/s. The initial temperature of the cooling fluid water is set at 28°C.

To improve the transparency and reproducibility of the CFD methodology, the numerical setup and validation strategy are reported in this study. This simulation was performed using ANSYS Fluent with a steady-state pressure-based solver and an absolute velocity formulation. The settings in this simulation are common to previous studies [27, 28] and include activation of the energy equation, while turbulence is modeled using the SST k-ω model. In addition, radiative heat transfer is considered using the Discrete Ordinates radiation model. For the numerical solution method, the pressure-velocity coupling is handled using the Coupled scheme. The spatial discretization scheme is defined as follows: Cell-Based Least Squares for gradient evaluation, Second Order for pressure, turbulent kinetic energy (k), specific dissipation rate (ω), and energy equations. Convergence is assessed using scaled residuals and stabilization of monitored thermal variables, including outlet water temperature and PV module temperature. The residual history shows a consistent reduction, with the energy residuals reaching the order of 10^{-6} and the other governing equations decreasing to quite low levels, indicating steady convergence of the numerical solution.

C. Grid Independence Test and Meshing Process

The purpose of the grid independence test is to ensure that the CFD simulation results are no longer dependent on the mesh density used. This test is essential for validating the numerical accuracy of the model before the main simulation is performed. The results of the grid independence test are shown in Figure 3.

The grid size variations used in the simulation ranged from 3.9 mm to 9 mm, or from approximately 170,000 to 790,000 mesh elements. The results showed that the average PV temperature stabilized after passing 256,000 mesh elements at a temperature of 51.9 °C.

All three PVT systems use the hex-dominant method for meshing with an element size of 5 mm. The twin spiral design has 577,763 nodes and 355,034 elements. The direct design has 577,857 nodes and 343,925 elements. For the oscillatory design, there are 559,682 nodes and 344,363 elements.

D. Energy Analysis

Thermal efficiency and electrical efficiency are the two main metrics used to evaluate a PVT system's performance. The study utilized ANSYS Fluent to acquire the results of the numerical analysis conducted under steady-state conditions. These results included the surface temperature of the PV module and the temperature of the outflow water. The thermal energy recovered from the collector is defined as the rate at which the fluid absorbs heat:

$$Q_u = \dot{m}C_p(T_o - T_i) \quad (1)$$

where C_p and $\dot{m}$ denote the water heat capacity and the mass flow rate, respectively. During simulation, T_o and T_i denote the water output and intake temperature, respectively. The thermal efficiency is then normalized against the radiation entering the collector surface [29]:

$$\eta_{th} = \frac{Q_u}{GA_c} \quad (2)$$

where η_{th} is the solar collector thermal efficiency, Q_u is the usable heat gain, G is the solar irradiance, and A_c is the PVT collector area.

The PVT system electrical efficiency (η_{el}) is determined using [30]:

$$\eta_{el} = \eta_r(1-\gamma(T_c - T_r)) \quad (3)$$

where T_r and T_c represent the reference temperature and the cell temperature, γ is the temperature coefficient (γ = 0.0041 °C^{-1}), η_r is the PV reference efficiency (η_r = 0.12), and η_{el} is the electrical efficiency PV.

III. RESULTS AND DISCUSSION

A. Contour Temperature Distribution on Collector

The simulation results obtained using ANSYS Fluent show the fluid temperature distribution in the PVT collector channel with three configurations, namely twin spiral, direct, and oscillatory. Figure 4 displays the temperature distribution contour in the PVT collector absorber with three different configurations at a mass flow rate of 0.02 kg/s, an inlet water temperature of 28 °C, and a solar radiation level of 900 W/m².

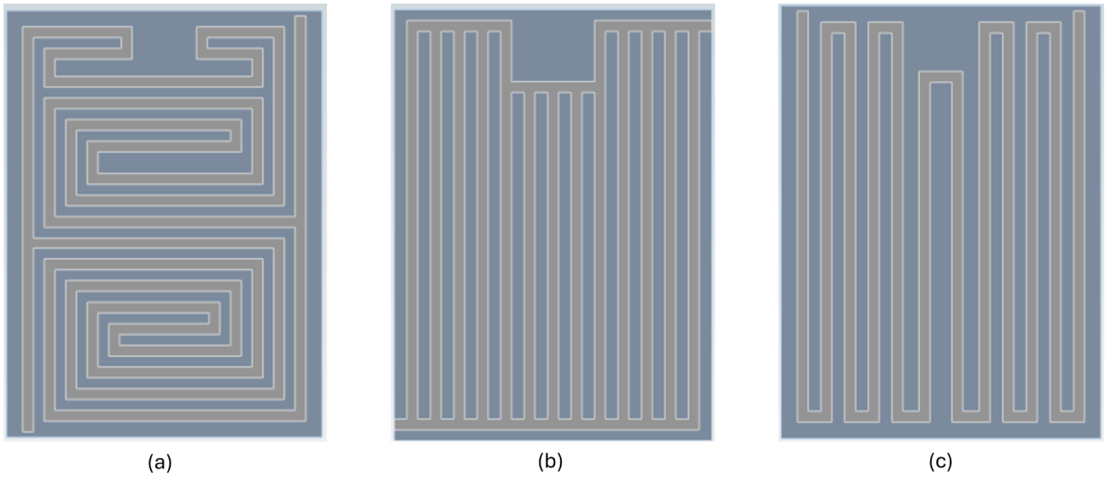

Fig. 2. Different collector configurations: (a) twin spiral, (b) direct, and (c) oscillatory.

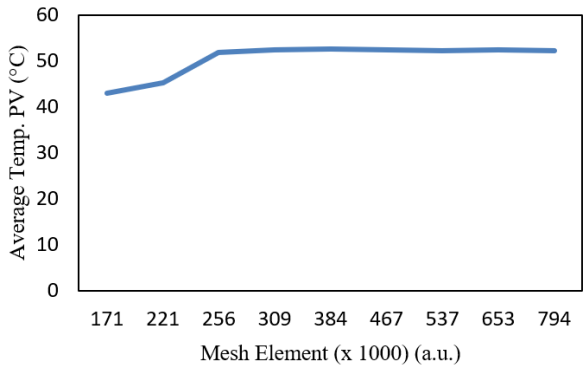

Fig. 3. Grid independence test for average PV temperature for mesh element counts ranging from 170,000 – 790,000.

As illustrated in Figure 4, the collector absorber configuration has a strong influence on the spatial temperature distribution of the PVT collector. The direct configuration (Figure 4(b)) presents a highly non-uniform thermal field, characterized by a concentrated high-temperature zone in the middle channels (approximately 40.6–42.0 °C) and comparatively cooler regions near the channel extremities (approximately 28–32 °C). The average outlet water temperature reaches 37.46 °C. This pattern indicates uneven heat extraction and a greater tendency towards thermal concentration.

In comparison, the twin spiral configuration (Figure 4(a)) exhibits a more homogeneous contour distribution, with most of the collector area remaining within a relatively narrow temperature band (approximately 31–39 °C) and an average outlet water temperature of 36.11 °C. The oscillatory configuration (Figure 4(c)) also shows improved thermal distribution relative to the direct channel, with temperatures generally distributed within 30–39 °C and an average outlet water temperature of 35.08 °C, although a moderate temperature gradient is still observed along the flow path. These contour-based observations provide qualitative support for the quantitative results, where the twin spiral and oscillatory configurations achieve better PV cooling performance than the direct configuration.

B. Contour Temperature Distribution on the PV Module Surface

Figure 5 presents the surface temperature contours of the PV module for each absorber collector configuration under a solar radiation of 900 W/m², an inlet water temperature of 28 °C, and a water mass flow rate of 0.02 kg/s.

The direct configuration (Figure 5 (b)) exhibits the most pronounced non-uniform temperature distribution, with a distinct high-temperature region concentrated in the central part of the PV surface. Based on the contour scale, the local PV surface temperature in this region reaches approximately 55–62 °C, while cooler regions near the inlet-side channels remain around 34–45 °C, indicating uneven cooling and a higher risk of localized hotspot formation. The average temperature of the PV module is 56.59 °C.

In contrast, the twin spiral configuration (Figure 5 (a)) demonstrates a more homogeneous surface-temperature distribution, with most of the PV area remaining within a narrower range of approximately 44–56 °C, and with no dominant hotspot concentrated in a single region. This contour pattern suggests more effective heat spreading and more uniform convective heat removal across the PV module surface. The average temperature at the PV module surface is 56.59 °C.

The oscillatory configuration (Figure 5 (c)) also improves the PV surface temperature distribution compared with the direct configuration. Although a warmer region is still visible along part of the channel path, the thermal field is more evenly distributed than in the direct case, with the PV surface temperature generally ranging from approximately 40–58 °C. Thus, the oscillatory design reduces thermal non-uniformity relative to the direct configuration, but the twin spiral configuration remains the most uniform.

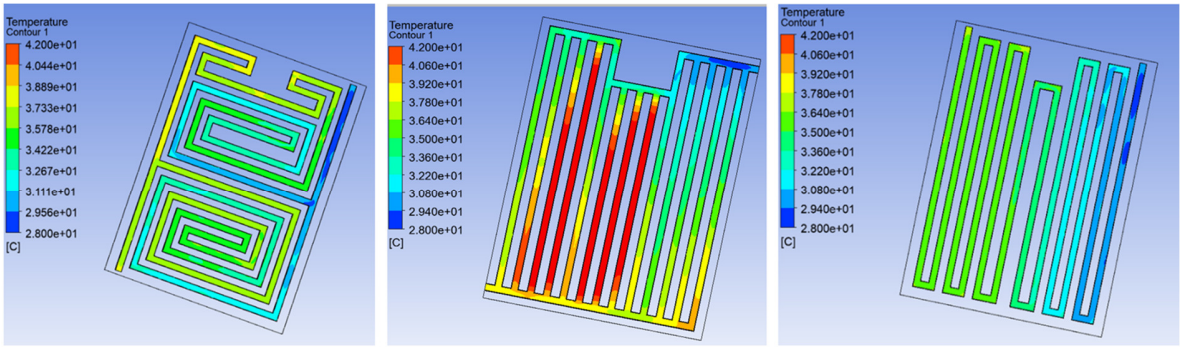

(a) (b) (c)

Fig. 4. Temperature contour plots of PVT collector: (a) twin spiral, (b) direct, and (c) oscillatory at an irradiance of 900 W/m² and a mass flow rate of 0.02 kg/s.

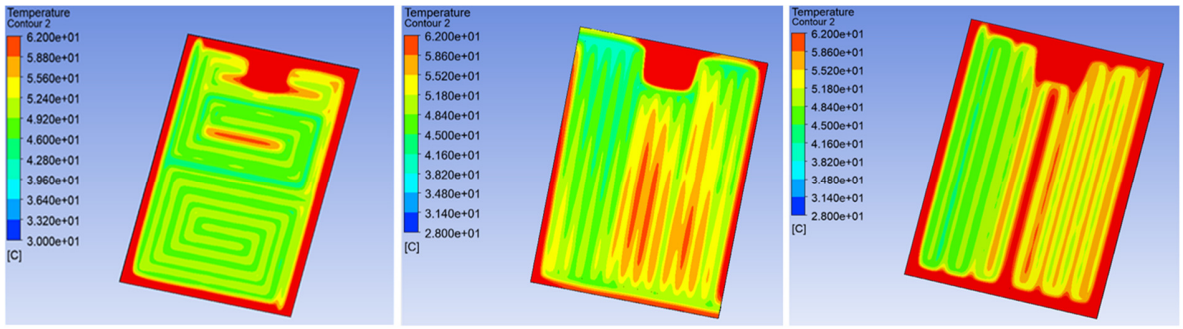

(a) (b) (c)

Fig. 5. Temperature contour plots of the PV module surface: (a) twin spiral, (b) direct, and (c) oscillatory at an irradiance of 900 W/m² and a mass flow rate of 0.02 kg/s.

C. Electrical Performance of the PVT Collector

Figure 6 depicts the simulation results for several PVT collector configurations under variations in water mass flow rate (0.015 kg/s – 0.055 kg/s) at a radiation level of 900 W/m², which affects the temperature of the PV module and electrical efficiency. More detailed results under different levels of solar radiation with several solar collector configurations are presented in Tables II - V.

Figure 6 generally shows two main trends: a decrease in PV module temperature and an increase in electrical efficiency with increasing mass flow rate. At low mass flow rates (approximately 0.015–0.02 kg/s), all configurations exhibit relatively high module temperatures. The direct configuration produces the highest temperature, reaching approximately 60 °C, followed by the oscillatory (45°C) and the twin spiral configuration (43°C). When the mass flow rate is increased to 0.05 kg/s, a significant temperature decrease occurs in all three configurations. The direct configuration shows a decrease to approximately 49°C, whereas the twin spiral and oscillatory configurations maintain module temperatures in the range of 39–42°C. This phenomenon indicates that increasing the mass flow rate enhances the fluid's ability to absorb and transport heat from the bottom surface of the PV module. However, at flow rates above 0.03 kg/s, the temperature drop tends to slow, indicating that the heat transfer process has approached saturation.

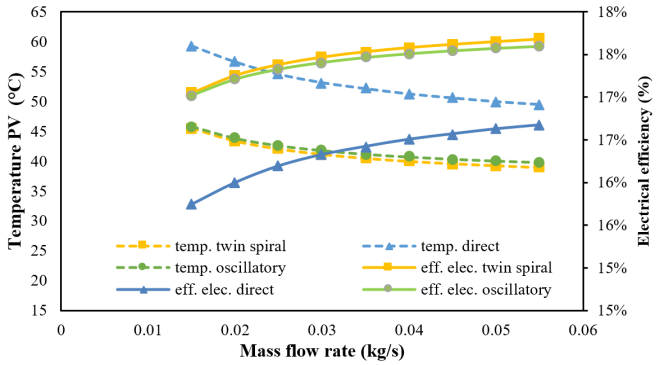

Fig. 6. Effect of mass flow rate on PV module temperature and electrical efficiency for different collector configurations at 900 W/m².

Based on Tables II - V, the results show that increasing the fluid mass flow rate is inversely proportional to the PV module temperature and directly proportional to the increase in electrical efficiency. Conversely, increasing solar radiation intensity causes an increase in module temperature and a decrease in electrical efficiency.

TABLE II. PV TEMPERATURE AND PV EFFICIENCY UNDER VARIOUS MASS FLOW RATES AT A SOLAR IRRADIANCE OF 1000 W/m²

$\dot{m}$	Twin spiral		Direct		Oscillatory	
(kg/s)	Tpv (°C)	Eff. PV	Tpv (°C)	Eff. PV	Tpv (°C)	Eff. PV
0.015	47.61	16.85%	63.05	15.39%	48.01	16.81%
0.02	45.19	17.08%	60.05	15.67%	45.77	17.03%
0.025	43.69	17.22%	57.99	15.87%	44.39	17.16%
0.03	42.67	17.32%	56.48	16.01%	43.44	17.25%
0.035	41.92	17.39%	55.32	16.12%	42.75	17.31%
0.04	41.36	17.45%	54.43	16.20%	42.23	17.36%
0.045	40.91	17.49%	53.60	16.28%	41.81	17.40%
0.05	40.54	17.52%	52.93	16.35%	41.47	17.44%
0.055	40.20	17.56%	52.37	16.40%	41.19	17.46%

TABLE III. PV TEMPERATURE AND PV EFFICIENCY UNDER VARIOUS MASS FLOW RATES AT A SOLAR IRRADIANCE OF 900 W/m²

$\dot{m}$	Twin spiral		Direct		Oscillatory	
(kg/s)	Tpv (°C)	Eff. PV	Tpv (°C)	Eff. PV	Tpv (°C)	Eff. PV
0.015	45.56	17.05%	59.29	15.74%	45.85	17.02%
0.02	43.38	17.25%	56.60	16.00%	43.85	17.21%
0.025	42.05	17.38%	54.53	16.19%	42.61	17.33%
0.03	41.12	17.47%	53.13	16.33%	41.78	17.41%
0.035	40.46	17.53%	52.12	16.42%	41.16	17.46%
0.04	39.95	17.58%	51.24	16.51%	40.70	17.51%
0.045	39.55	17.62%	50.57	16.57%	40.33	17.54%
0.05	39.22	17.65%	49.95	16.63%	40.03	17.57%
0.055	38.90	17.68%	49.47	16.67%	39.78	17.60%

TABLE IV. PV TEMPERATURE AND PV EFFICIENCY UNDER VARIOUS MASS FLOW RATES AT A SOLAR IRRADIANCE OF 700 W/m²

$\dot{m}$	Twin spiral		Direct		Oscillatory	
(kg/s)	Tpv (°C)	Eff. PV	Tpv (°C)	Eff. PV	Tpv (°C)	Eff. PV
0.015	41.23	17.46%	51.32	16.50%	41.41	17.44%
0.02	39.60	17.61%	48.99	16.72%	39.95	17.58%
0.025	38.59	17.71%	47.56	16.86%	39.04	17.67%
0.03	37.92	17.77%	46.47	16.96%	38.41	17.73%
0.035	37.42	17.82%	45.75	17.03%	37.95	17.77%
0.04	37.03	17.86%	45.16	17.08%	37.60	17.80%
0.045	36.72	17.89%	44.71	17.13%	37.32	17.83%
0.05	36.47	17.91%	44.37	17.16%	37.09	17.85%
0.055	36.26	17.93%	44.07	17.19%	36.90	17.87%

TABLE V. PV TEMPERATURE AND PV EFFICIENCY UNDER VARIOUS MASS FLOW RATES AT A SOLAR IRRADIANCE OF 600 W/m²

$\dot{m}$	Twin spiral		Direct		Oscillatory	
(kg/s)	Tpv (°C)	Eff. PV	Tpv (°C)	Eff. PV	Tpv (°C)	Eff. PV
0.015	39.11	17.66%	47.40	16.87%	39.16	17.65%
0.02	37.73	17.79%	45.58	17.05%	37.96	17.77%
0.025	36.86	17.87%	44.16	17.18%	37.20	17.84%
0.03	36.29	17.93%	43.36	17.26%	36.69	17.89%
0.035	35.86	17.97%	42.76	17.31%	36.31	17.93%
0.04	35.53	18.00%	42.35	17.35%	36.01	17.95%
0.045	35.28	18.02%	42.03	17.38%	35.77	17.98%
0.05	35.07	18.04%	41.74	17.41%	35.57	18.00%
0.055	34.91	18.06%	41.49	17.43%	35.40	18.01%

Across all solar radiation levels, a consistent trend indicates that increasing the mass flow rate from 0.015 kg/s to 0.055 kg/s results in a significant decrease in PV module temperature. For example, at a solar radiation intensity of 1000 W/m² (Table II), the twin spiral configuration shows a decrease in Tpv from 47.61°C to 40.20°C, with an increase in electrical efficiency from 16.85% to 17.56%. This phenomenon is caused by the increased convective heat transfer rate between the absorber surface and the cooling fluid, which accelerates heat dissipation from the solar cell and reduces internal resistance due to the temperature increase. This impact implies a higher electrical conversion efficiency. Reducing the irradiance from 1000 W/m² to 600 W/m² consistently decreased the PV module temperature for each configuration and mass flow rate. This decrease occurred due to the reduced heat energy absorbed by the module surface, thereby reducing heat accumulation in the absorber layer.

Comparative results show that the twin spiral configuration consistently provided the lowest module temperature and the highest electrical efficiency across all variations in irradiance and mass flow rates. For example, at an intensity of 900 W/m² with a flow rate of 0.055 kg/s, the twin spiral configuration achieved a Tpv of 38.90°C and an efficiency of 17.60%, while the direct and oscillatory configurations produced Tpvs of 41.69°C and 39.78°C, respectively, with lower efficiencies. This demonstrates that the twin spiral flow design offers more effective cooling capabilities due to its turbulence and increased heat transfer area.

D. Thermal Performance of the PVT Collector

Figure 7 illustrates the impact of the changes in water mass flow rate on outlet water temperature and thermal efficiency at a radiation level of 900 W/m².

Based on the simulation results (Figure 7), there is an inverse correlation between the water mass flow rate and the outlet water temperature. At a radiation level of 900 W/m², along with an increase in the mass flow rate of water from 0.015 kg/s to 0.055 kg/s, the outlet water temperature decreases for all three configuration types. With this flow rate, the oscillatory configuration achieves the lowest outlet water temperature from 37.75 °C to 29.98 °C, for the twin spiral configuration from 39.19 °C to 30.4 °C, whereas for the direct configuration from 40.99 °C to 31.07 °C. This effect is very significant at lower mass flow rates and tends to slope at higher rates. The impact of different mass flow rates on thermal, electrical, and total PVT efficiencies for the three collector configurations is portrayed in Figure 8. In general, increasing the mass flow rate results in a rising trend in electrical, thermal, and total PVT efficiency. At a mass flow rate of 0.02 kg/s, the direct configuration provides the highest thermal efficiency (77.44%), followed by the twin spiral (77.37%) and the oscillatory (77.35%). The electrical efficiency of the twin spiral configuration (17.25%) is slightly higher than that of the oscillatory (17.21%) and direct (16%) configurations. This indicates that the cooling mechanism in the twin spiral configuration is more effective in reducing the temperature of the PV cell, thereby increasing the performance of electrical energy conversion. Overall, the combination of thermal and electrical efficiency affects the total PVT efficiency. The twin

spiral configuration produces the highest total efficiency (94.62%), followed by oscillatory (94.56%), whereas the direct configuration is slightly lower (93.44%).

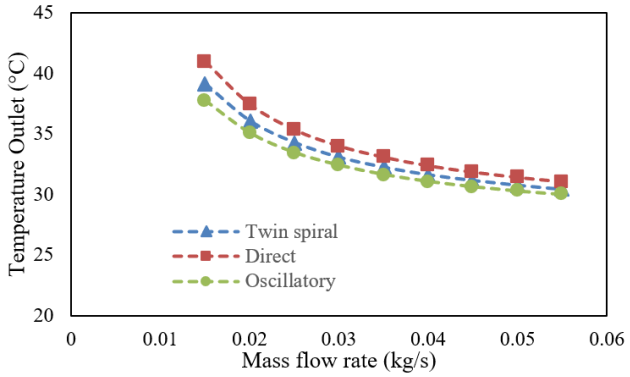

Fig. 7. The influence of different mass flow rates on water outlet temperature at different collector configurations under 900 W/m² solar irradiance.

Validation evidence is provided by the PVT study conducted in [28]. Authors in [28] reported an average deviation of 5.1% for thermal efficiency and 3.7% for electrical efficiency between the numerical and experimental results. In Figure 9, it can be observed that the effect of increasing mass flow rate on PV temperature in the present study and in [28] shows an identical trend. Quantitatively, the deviation between the present study and the reference data ranges from 4.73% to 7.47%, with an average percentage deviation of 6.91% and an average absolute deviation of 2.69 °C. The present study consistently predicts slightly lower PV temperatures than those reported in [28], with differences ranging from 1.94 to 2.89 °C. Nevertheless, the overall agreement indicates that the adopted numerical model can reproduce the thermal behavior of the PVT system with reasonable accuracy.

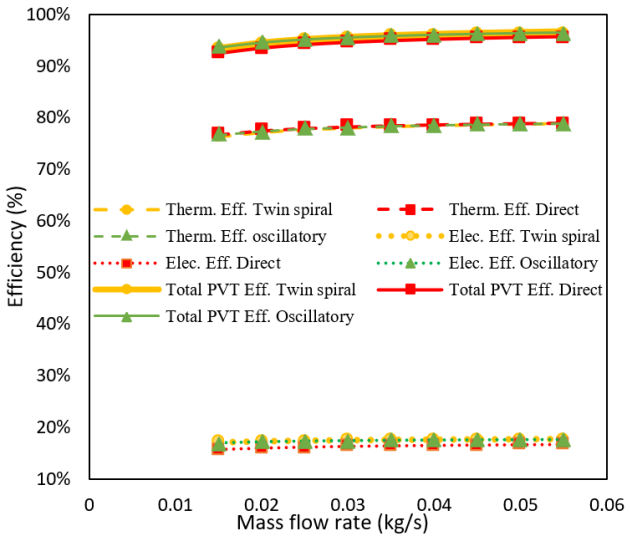

Fig. 8. The influence of mass flow rate on electrical, thermal, and PVT efficiencies across various collector configurations at 900 W/m².

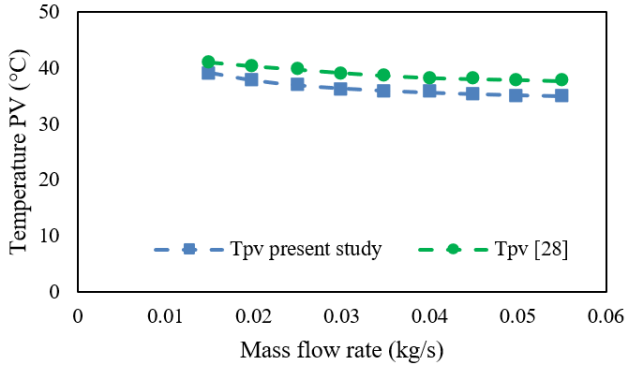

Fig. 9. Comparison of PV temperature between the present study and the published data reported in [28] at different mass flow rates under an irradiance of 600 W/m².

IV. CONCLUSIONS

The present study evaluated the performance of Photovoltaic Thermal (PVT) collectors with different collector configurations, namely twin spiral, direct, and oscillatory. Simulations were carried out by considering the effect of different water mass flow rates and variation in solar irradiance. The results indicate that collector configuration plays a key role not only in heat absorption but also in temperature uniformity on the PV module surface. Among the three configurations, the twin spiral configuration provided the best overall performance. At 900 W/m² and 0.02 kg/s, it reduced the PV temperature to 43.38 °C, compared with 56.59 °C for the direct configuration and 43.84 °C for the oscillatory configuration. Under the same condition, the twin spiral configuration achieved an electrical efficiency of 17.25% and a thermal efficiency of 77.37%, compared with 16.00% and 77.44% for the direct configuration, and 17.21% and 77.35% for the oscillatory configuration.

From a practical engineering perspective, the twin spiral configuration can be considered the most advantageous choice for water-based PV systems, especially in hot climates. This is due to its ability to maintain a balance between thermal and electrical performance and to produce a more even cooling distribution across the module. Meanwhile, the oscillatory configuration can still be considered a viable alternative, especially if a slight performance reduction is tolerable for ease of design or manufacturing. Conversely, the direct configuration tends to be less suitable for applications where stable electrical output is a top priority. Nevertheless, this study is subject to several limitations. The analysis was conducted under steady-state Computational Fluid Dynamics (CFD) simulations and did not include exergy analysis, pumping power assessment, or economic evaluation. Future research should therefore incorporate transient analysis under real-world operating conditions and integrated exergy–economic analyses, together with hydraulic performance evaluation, to further optimize collector absorber design and support large-scale implementation.

DECLARATION OF COMPETING INTERESTS

The authors declare the absence of any functional or financial conflicts that could potentially interfere with the integrity of this paper.

ACKNOWLEDGMENT

The authors gratefully acknowledge the financial support for the Article Processing Charge (APC) provided by the Unit of Research, Innovation, and Community Engagement, Faculty of Engineering, Universitas Indonesia (2026) under contract No. NKB-1129/UN2.F4.D/PPM.00.04/2026.

DATA AVAILABILITY

The datasets generated and analyzed during this research are fully documented in the manuscript.

REFERENCES

[1] R. Karmakar, V. Tripathi, P. Kumar, N. Singh, and R. Kumar, "The Interplay of Fossil Fuels and Natural Disasters", in *Climate Crisis and Sustainable Solutions: Strategies for Adaptation, Mitigation and Sustainable Development*, N. Singh and S. A. Babu, Eds. Singapore: Springer Nature, 2024, ch. 6, pp. 91–106.

[2] S. E. Hosseini, "Fossil fuel crisis and global warming," in *Fundamentals of Low Emission Flameless Combustion and Its Applications*, S. E. Hosseini, Ed., 1st ed. London, United Kingdom: Academic Press, 2022, ch. 1, pp. 1–11.

[3] G. Nagababu, V. S. K. V. Harish, K. Doshi, Y. Bhat, and M. Bansal, "Harnessing Solar Energy for Sustainable Development of Livelihoods," in *Handbook of Climate Change Mitigation and Adaptation*, M. Lackner, B. Sajjadi, and W.-Y. Chen, Eds., 3rd ed. Cham: Springer International Publishing, 2022, pp. 1249–1284, https://doi.org/10.1007/978-3-030-72579-2_113.

[4] H. M. Wassie, K. E. Kassie, and M. Z. Getie, "A Comprehensive Review on the Photovoltaic Panel Cooling Technique for Improved Efficiency," in *Sustainable Development Research in Materials and Renewable Energy Engineering: Advancements of Science and Technology*, M. Z. Getie, K. Mequanint, M. A. Alemu, G. Y. Ashebir, and M. T. Tigabu, Eds. Cham: Springer Nature Switzerland, 2025, pp. 369–392.

[5] S. S. Das, P. Kumar, and S. S. Sandhu, "Hybrid photovoltaic–thermal system for simultaneous generation of power and hot water utilising mobiltherm as heat transfer fluid," *International Journal of Sustainable Energy*, vol. 40, no. 2, pp. 104–119, 2021, https://doi.org/10.1080/14786451.2020.1798959.

[6] A. Miglioli, N. Aste, C. Del Pero, and F. Leonforte, "Photovoltaic-thermal solar-assisted heat pump systems for building applications: Integration and design methods," *Energy and Built Environment*, vol. 4, no. 1, pp. 39–56, Feb. 2023, https://doi.org/10.1016/j.enbenv.2021.07.002.

[7] A. Gagliano and S. Aneli, "Energy analysis of hybrid solar thermal plants (PV/T)," in *Recent Advances in Renewable Energy Technologies*, 1st ed. London. United Kingdom: Academic Press, 2021, ch. 2, pp. 45–90, https://doi.org/10.1016/B978-0-323-91093-4.00003-2.

[8] A. Z. V. Bonilla *et al*., "Systematic Review of Flat Plate Photovoltaic Thermal Systems: Components, Efficiency, Monitoring, and Artificial Intelligence," *Energy Technology*, vol. 13, no. 11, 2025, Art. no. 2500425, https://doi.org/10.1002/ente.202500425.

[9] S. Abdul-Ganiyu, D. A. Quansah, E. W. Ramde, R. Seidu, and M. S. Adaramola, "Techno-economic analysis of solar photovoltaic (PV) and solar photovoltaic thermal (PVT) systems using exergy analysis," *Sustainable Energy Technologies and Assessments*, vol. 47, Oct. 2021, Art. no. 101520, https://doi.org/10.1016/j.seta.2021.101520.

[10] Y. E. Alami *et al*., "Comparative study of the performance of photovoltaic and photovoltaic thermal solar systems: Case study in El Jadida," *E3S Web of Conferences*, vol. 601, 2025, Art. no. 00011, https://doi.org/10.1051/e3sconf/202560100011.

[11] H. A. Al-zurfi, H. H. Balla, A. N. Al-Shamani, and A. M. Hayder, "Numerical Study to Enhance The Electrical And Thermal Efficiency Of PV/T System," *IOP Conference Series: Materials Science and Engineering*, vol. 928, no. 2, 2020, Art. no. 022136, https://doi.org/10.1088/1757-899X/928/2/022136.

[12] N. F. M. Razali, A. Fudholi, M. H. Ruslan, and K. Sopian, "Improvement of photovoltaic module efficiency using spiral absorber and water," *Journal of Advanced Research in Fluid Mechanics and Thermal Sciences*, vol. 73, no. 1, pp. 131–139, 2020, https://doi.org/10.37934/arfmts.73.1.131139.

[13] E. E. H. O. Swese *et al*., "Improving Thermal and Electricity Generation Performance of Photovoltaic/Thermal (PV/T) Systems Using Hybrid Nanofluid," *Heat Transfer Research*, vol. 55, no. 8, 2024, https://doi.org/10.1615/HeatTransRes.2023049992.

[14] J. Walshe, J. Doran, and G. Amarandei, "Evaluation of the potential of nanofluids containing different Ag nanoparticle size distributions for enhanced solar energy conversion in hybrid photovoltaic-thermal (PVT) applications," *Nano Express*, vol. 3, no. 1, Jan. 2022, Art. no. 015001, https://doi.org/10.1088/2632-959X/ac49f2.

[15] D. Kumar Sharma, V. S., P. V. Bhale, and M. K. Rathod, "Analysis of water and refrigerant-based PV/T systems with double glass PV modules: An experimental and computational approach," *Solar Energy*, vol. 268, Jan. 2024, Art. no. 112296, https://doi.org/10.1016/j.solener.2023.112296.

[16] I. Karaaslan and T. Menlik, "Numerical study of a photovoltaic thermal (PV/T) system using mono and hybrid nanofluid," *Solar Energy*, vol. 224, pp. 1260–1270, Aug. 2021, https://doi.org/10.1016/j.solener.2021.06.072.

[17] A. Kazemian, M. Hosseinzadeh, M. Sardarabadi, and M. Passandideh-Fard, "Effect of glass cover and working fluid on the performance of photovoltaic thermal (PVT) system: An experimental study," *Solar Energy*, vol. 173, pp. 1002–1010, Oct. 2018, https://doi.org/10.1016/j.solener.2018.07.051.

[18] K. D. Arvanitis, E. Papanicolaou, E. Mathioulakis, V. Belessiotis, and D. Bouris, "Experimental evaluation of flat-plate heat absorbers for medium-temperature linear-focus solar systems: Composite U-bends vs straight rectangular-multi-channels," *Applied Thermal Engineering*, vol. 175, July 2020, Art. no. 115364, https://doi.org/10.1016/j.applthermaleng.2020.115364.

[19] A. Seddaoui, M. Z. Dar Ramdane, and R. Noureddine, "Performance investigation of a new designed vacuum flat plate solar water collector: A comparative theoretical study," *Solar Energy*, vol. 231, pp. 936–948, Jan. 2022, https://doi.org/10.1016/j.solener.2021.12.038.

[20] Z. Wang, G. Hou, H. Taherian, and Y. Song, "Numerical Investigation of Innovative Photovoltaic–Thermal (PVT) Collector Designs for Electrical and Thermal Enhancement," *Energies*, vol. 17, no. 10, Jan. 2024, Art. no. 2429, https://doi.org/10.3390/en17102429.

[21] A. Almalih, A. K. Azab, and M. E. ElRefaie, "An Experimental Investigation of Optimizing a Water-Based Photovoltaic Thermal (PVT) System through Reduced Tube Spacing," *Engineering, Technology & Applied Science Research*, vol. 15, no. 5, pp. 26323–26329, Oct. 2025, https://doi.org/10.48084/etasr.12227.

[22] A. Sharma, S. Thakur, P. Dhiman, and A. Deshta, "Augmentation of heat transmission in solar collectors with jet impingement: a review," *International Journal of Ambient Energy*, vol. 46, no. 1, Dec. 2025, Art. no. 2495816, https://doi.org/10.1080/01430750.2025.2495816.

[23] H. Liu and W. Zhu, "Optimisation analysis by numerical simulation of adding internal fins in photovoltaic/thermal system based on Taguchi method," *Applied Thermal Engineering*, vol. 266, May 2025, Art. no. 125635, https://doi.org/10.1016/j.applthermaleng.2025.125635.

[24] A. Kazemian, T. Ma, and Y. Hongxing, "Evaluation of various collector configurations for a photovoltaic thermal system to achieve high performance, low cost, and lightweight," *Applied Energy*, vol. 357, Mar. 2024, Art. no. 122422, https://doi.org/10.1016/j.apenergy.2023.122422.

[25] H. A. Kazem, A. H. A. Al-Waeli, M. T. Chaichan, K. H. Al-Waeli, A. B. Al-Aasam, and K. Sopian, "Evaluation and comparison of different flow configurations PVT systems in Oman: A numerical and experimental investigation," *Solar Energy*, vol. 208, pp. 58–88, Sept. 2020, https://doi.org/10.1016/j.solener.2020.07.078.

[26] U. Olmuş, Y. E. Güzelel, K. N. Çerçi, and O. Büyükalaca, "Numerical analysis and comparison of different serpentine-based photovoltaic-thermal collectors," *Renewable Energy*, vol. 241, Mar. 2025, Art. no. 122196, https://doi.org/10.1016/j.renene.2024.122196.

[27] J. Lukasik and J. Wajs, "Experimental and numerical study of thermal and electrical potential of BIPV/T collector in the form of air-cooled photovoltaic roof tile," *International Journal of Heat and Mass Transfer*, vol. 227, Aug. 2024, Art. no. 125554, https://doi.org/10.1016/j.ijheatmasstransfer.2024.125554.

[28] B. Yan *et al*., "Numerical and Experimental Investigation of Photovoltaic/Thermal Systems: Parameter Analysis and Determination of Optimum Flow," *Sustainability*, vol. 14, no. 16, 2022, Art. no. 10156, https://doi.org/10.3390/su141610156.

[29] H. Ren, Y. Li, W. Lin, and Y. Sun, "Energy and economic analysis of photovoltaic thermal night cooling and adaptive reset control for ultra-efficient data center immersion cooling," *Renewable Energy*, vol. 255, Dec. 2025, Art. no. 123821, https://doi.org/10.1016/j.renene.2025.123821.

[30] N. Liu, D. Jiang, H. Liu, K. Sun, and S. Bai, "Experimental and simulation study on a novel photovoltaic-thermal (PVT) system with enhanced combined thermal and electrical efficiency," *Energy Sources, Part A: Recovery, Utilization, and Environmental Effects*, vol. 47, no. 1, pp. 12059–12076, 2025, https://doi.org/10.1080/15567036.2025.2505971.